



www.chemeurj.org

# Contrasting Reactions of Carbodiimides with Divalent Lanthanoid Species

Vidushi P. Vithana, [a] Zhifang Guo, [a] Glen B. Deacon, [b] and Peter C. Junk\*[a]

Reactions of lanthanoid species with carbodiimides (RN = C = NR') show considerable variety. Thus, treatment of the divalent 2,6-di-*tert*-butyl-4-ethylphenolatosamarium complex, [Sm(OAr<sup>Et</sup>)<sub>2</sub>(thf)<sub>3</sub>]-PhMe with *N,N'*-diisopropylcarbodiimide (*iP*rNCN*iP*r) resulted in the formation of the oxalamidinatosamarium(III) complex [(OArEt)<sub>2</sub>Sm( $\mu$ -C<sub>2</sub>N<sub>4</sub>*iP*r<sub>4</sub>)Sm(OAr<sup>Et</sup>)<sub>2</sub>]-2PhMe (1). In contrast, the use of the bulkier *N,N'*-dicyclohexylcarbodiimide (CyNCNCy) led to the formation of a formamidinatosamarium(III) complex [Sm(OAr<sup>Et</sup>)<sub>2</sub>(CyNC(H)NCy)(thf)<sub>2</sub>]-2thf (2). Reactions between rare earth metals (RE = Yb, Eu) with one

molar equivalent of bis(phenylethynyl)mercury (Hg(PhCC) $_2$ ) and two molar equivalents of N,N'-dicyclohexylcarbodiimide (CyNCNCy) in tetrahydrofuran (thf) at room temperature yielded lanthanoid C-phenylethynylamidinate complexes, trivalent [Yb $^{||}$ {CyNC(C $\equiv$ CPh)NCy} $_3$ ]-2thf (3) and divalent [Eu{CyNC(C $\equiv$ CPh)NCy} $_2$ (thf) $_2$ ] (4). [Sm(OAr $^{Et}$ ) $_2$ (thf) $_3$ ].PhMe was obtained from Sml $_2$ (thf) $_2$  and the in situ generated potassium aryl oxide and is a five-coordinate monomer with a stereochemistry between trigonal bipyramidal and square pyramidal.

#### 1. Introduction

Carbodiimides (RN=C=NR') are important substrates in metal-based reactivity studies, leading to the formation of diverse range of coordination compounds with modified organic fragments.<sup>[1-6]</sup> These compounds serve as excellent building blocks for the synthesis of a wide range of complex organic compounds and are considered as one of the most important classes of nitrogen reagents due to their diverse chemical properties,<sup>[3,5-10]</sup> and are isoelectronic with CO<sub>2</sub>.

Carbodiimide insertion into metal–carbon sigma bonds forms amidinato complexes and they have been utilized in lanthanoid metal coordination chemistry, offering a route to lanthanoid amidinates. [11–13] Guanidinates, introduced in 1970, also form through carbodiimide insertion, specifically into Ln—N bonds of lanthanoid amides, yielding low-valent lanthanoid species. [14–17] Reductive coupling of carbodiimides with low-valent metal complexes has provided an exciting and straightforward reaction method, leading to novel metallocycles. Organosamarium(II) complexes, in particular, are strong reducing

agents that react with various unsaturated substrates, producing bimetallic complexes by reductive coupling reactions.<sup>[2,11,18–21]</sup>

In this study, contrasting reactions of unsaturated carbodiimide substrates (RN=C=NR') with Ln<sup>II</sup> aryloxides have been explored, offering a promising route to novel amidinatolanthanoid complexes. In addition, the reactivity of a carbodiimide with organolanthanoid alkynyl complexes generated by redox transmetallation, has been explored to examine insertion into Ln—C sigma bonds.

#### 2. Results and Discussion

#### 2.1. Synthesis

# 2.1.1. Reactions of carbodiimides with samarium(II) Bis(2,6-di-tert-butyl-4-ethylphenolate)

reaction of [Sm(OArEt)<sub>2</sub>(thf)<sub>3</sub>]·PhMe (preparation in Scheme 1) with an equivalent amount of N,N'-(iPrC=N=CiPr)diisopropylcarbodiimide (DIC) thf at room temperature resulted formation of the in the  $[(OAr^{Et})_2Sm(\mu$ oxalamidinatosamarium(III) complex  $C_2N_4iPr_4)Sm(OAr^{Et})_2]\cdot 2PhMe$  (1). Substituting the diisopropylcarbodiimide with the bulkier N,N'-dicyclohexylcarbodiimide (CyC=N=CCy) (DCC) gave the formamidinatosamarium(III) complex [Sm(OAr<sup>Et</sup>)<sub>2</sub>(CyNC(H)NCy)]·2thf (2) (Scheme 1). Furthermore, no evidence was found of competitive insertion of the carbodiimide into the Sm-O bond, probably owing to the oxophilicity of lanthanoids. The differing outcomes can be rationalized by 1 electron transfer to the carbodiimide forming a radical anion (species A in Scheme 1), which, for the less bulky carbodiimide, dimerizes to form the oxalamidinate ligand. The bulkier radical undergoes hydrogen abstraction from the solvent or reagents before dimerization can occur. H-abstraction from thf in

<sup>[</sup>a] V. P. Vithana, Z. Guo, P. C. Junk College of Science & Engineering, James Cook University, Townsville, Queensland 4811, Australia E-mail: peter.junk@jcu.edu.au

<sup>[</sup>b] G. B. Deacon School of Chemistry, Monash University, Clayton, Victoria 3800, Australia

Supporting information for this article is available on the WWW under https://doi.org/10.1002/chem.202500759

<sup>© 2025</sup> The Author(s). Chemistry – A European Journal published by Wiley-VCH GmbH. This is an open access article under the terms of the Creative Commons Attribution-NonCommercial-NoDerivs License, which permits use and distribution in any medium, provided the original work is properly cited, the use is non-commercial and no modifications or adaptations are made.

Scheme 1. Proposed reaction pathways leading to the formation of oxalamidinate (1) and formamidinate (2) complexes via reduction of carbodiimides by [Sm(OAr<sup>Et</sup>)<sub>2</sub>(thf)<sub>3</sub>]-PhMe.

lanthanoid chemistry has precedent.<sup>[22,23]</sup> This outcome is simpler than when H-abstraction occurs from the methine moiety of the diisopropyl group, which leads to coupling through the methine carbons.<sup>[2]</sup>

Fresh samples of compounds 1 and 2 gave satisfactory %Sm values, whilst microanalyses after transport to the UK showed loss of 1 toluene of crystallization and two thf of crystallization from the crystal composition of 1 and 2, respectively. The solvent loss was also detected by <sup>1</sup>H NMR spectroscopy (see Section 6). 2 also gave a low %C, a common issue with rare-earth metalorganic compounds.<sup>[24–30]</sup> The <sup>1</sup>H NMR spectrum of 1 is shifted from the normal diamagnetic region due to the paramagnetic Sm<sup>|||</sup> ion. The spectrum of 1 is complex, with the t-butyl resonances appearing as three sharp singlets at -0.79, -0.64, and -0.42 ppm, integrating overall to 72 hydrogens. The isopropyl CH<sub>3</sub> protons, along with the CH<sub>3</sub> resonances from the ethyl substituent on the OArEt group, are spread over a wide chemical shift range of 0.30-2.04 ppm. Only one lattice toluene molecule is observed in the proton NMR spectrum (Figure S1). In the 1H NMR spectrum of complex 2, signal broadening occurs due to the paramagnetic Sm<sup>III</sup> ion, complicating assignment and integration, especially in the upfield region. A pronounced downfield shift is observed for the formamidinate backbone NCHN, which appears as a singlet at  $\delta = 7.98$  ppm. The singlet at  $\delta =$ 8.15 ppm is assigned to the aromatic CH protons of the phenyl ring. Coordinated thf CH<sub>2</sub> signals are expected in the broad upfield region, but no lattice thf was detected in the proton NMR spectrum (Figure S2).

# 2.1.2. The one pot reactions of Ln metals with $Hg(PhCC)_2$ and N,N'-dicyclohexylcarbodiimide (CyNCNCy)

The reaction between an excess of rare earth metal, one molar equivalent of bis(phenylethynyl)mercury, and two molar equivalents of *N,N'*-dicyclohexylcarbodiimide (CyNCNCy) in tetrahydrofuran (thf) at room temperature gave amidinate complexes resulting from insertion of carbodiimide molecules into the Ln—C sigma bonds of Ln-CCPh species. The observed reactions are formulated in Scheme 2.

The reaction with Yb proceeds with the formation of yellow crystals of the homoleptic tris(amidinato) complex  $[Yb^{III}\{CyNC(C\equiv CPh)NCy\}_3]\cdot 2thf$  (3). As the redox transmetallation between Yb metal and  $Hg(CCPh)_2$  yields a divalent polymer  $[Yb(CCPh)_2]_{n,}^{[31]}$  the oxidation state outcome is unexpected, and a divalent complex analogous to 4 was anticipated. The formation of 3 is explicable if the expected  $[Yb(CyNC(C\equiv CPh)NCy)_2]$  is strongly reducing as it can then be oxidized by  $Hg(CCPh)_2$  to give a trivalent alkynyl  $[Yb(CyNC(C\equiv CPh)NCy)_2CCPh]$  into which a further carbodiimide can be inserted to give 3 (see Equations 1 and 2).

$$2 \left[ Yb\{CyNC(C \equiv CPh)NCy\}_{2} \right] + Hg(CCPH)_{2} \longrightarrow$$

$$2 \left[ Yb\{CyNC(C \equiv CPh)NCy\}_{2}(CCPH) \right] + Hg \tag{1}$$

There is precedent for reaction (1) in that the divalent Sm complex  $[Sm(DippForm)_2(thf)_2]$ , (DippFormH = N,N'-bis(2,6-diisopropylphenyl)formamidine), reacts with bis(phenylethynyl)mercury to give  $[Sm(DippForm)_2CCPh(thf)]$  with deposition of mercury metal. [23]

Elemental analyses of complexes **3** and **4** were consistent with the single crystal compositions. The  $^{1}H$  NMR spectrum of **3** exhibited broadening and shifting of signals due to the paramagnetism of Yb $^{|||}$ , making assignment and integration challenging, particularly in the upfield region. The cyclohexyl protons appeared alongside an additional 2.5 equivalents of thf from the solution, spanning a range of 3.94–1.50 ppm. The crystals were highly moisture sensitive and had to be quickly removed from the solution to ensure stability for NMR analysis. As a result, they retained 20 hydrogen atoms from residual free thf. The aromatic CH protons of the phenyl group were observed as two distinct resonances, one at 13.79 ppm, while the rest appeared over a range of 7.43–6.73 ppm, along with protons from  $C_6D_6$  solvent. A meaningful NMR spectrum could not be obtained for **4** because of paramagnetism. The most noteworthy features of the

28. Downloaded from https://chemistry-europe.onlinelibrary.wiley.com/doi/10.1002/chem.20200759 by James Cook University, Wiley Online Library on [23/11/2025]. See the Terms and Conditions

(https://onlinelibrary.wiley.com/terms-and-conditions) on Wiley Online Library for rules of use; OA articles are governed by the applicable Creative Commons License

Scheme 2. Synthesis of 3 and 4.

IR spectra of **3** and **4** are bands attributable to  $C \equiv C$  stretching at 2210–2120 cm<sup>-1</sup>.<sup>[32]</sup> Bands observed around 1500–1650 cm<sup>-1</sup> are assigned to delocalized C—N stretching vibrations.<sup>[33]</sup> The IR spectrum of **4** also displayed two distinct bands at 1043 and 886 cm<sup>-1</sup>, corresponding to coordinated thf.<sup>[34]</sup>

Several attempts were made to extend the study of Yb and Eu with N,N'-diisopropylcarbodiimide to establish a direct comparison with the Sm system. Unfortunately, none of these reactions produced crystals suitable for x-ray crystallography after trying many methods and solvents, so further studies were not conducted. Likewise, the reaction of Sm metal with  $Hg(CCPh)_2$  and either carbodiiomide did not have a satisfactory outcome.

#### 3. Molecular Structures

# 3.1. The complex $[(OAr^{Et})_2Sm(\mu-C_2N_4iPr_4)Sm(OAr^{Et})_2]-2PhMe$ (1)

Complex 1 crystallizes in the triclinic space group P-1, and the molecular structure adopts a diamidinate configuration. Each Sm atom is bound to opposing sides of the tetraisopropyloxalamidinate  $((iPr)_2N_2C-CN_2(iPr)_2^{2-})$  ligand, which functions as a bridging tetradentate ligand by chelating both Sm atoms

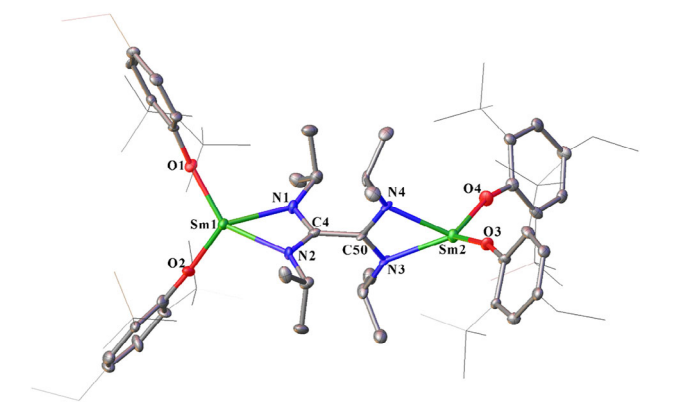


**Figure 1.** Molecular diagram of complex 1. Hydrogen atoms and the two lattice toluene molecules are omitted for clarity. *Tert*-butyl and ethyl groups are drawn as wireframe for clarity. Selected bond lengths (Å): C4–C50 1.488(17), N1–C4 1.370(15), N2–C4 1.337(16), N4–C50 1.378(15), N3–C50 1.288(15), Sm1–N1 2.364(11), Sm1–N2 2.416(10), Sm2–N4 2.36(1), Sm2–N3 2.382(10), Sm1–O1 2.090(8), Sm1–O2 2.063(9), Sm2–O3 2.140(9), Sm2–O4 2.115(9).

(Sm1 and Sm2) through four nitrogen atoms (N1, N2, N3, N4) (Figure 1). Two OAr<sup>Et</sup> ligands coordinate to each metal, giving the Sm atoms a coordination number of four (binding through



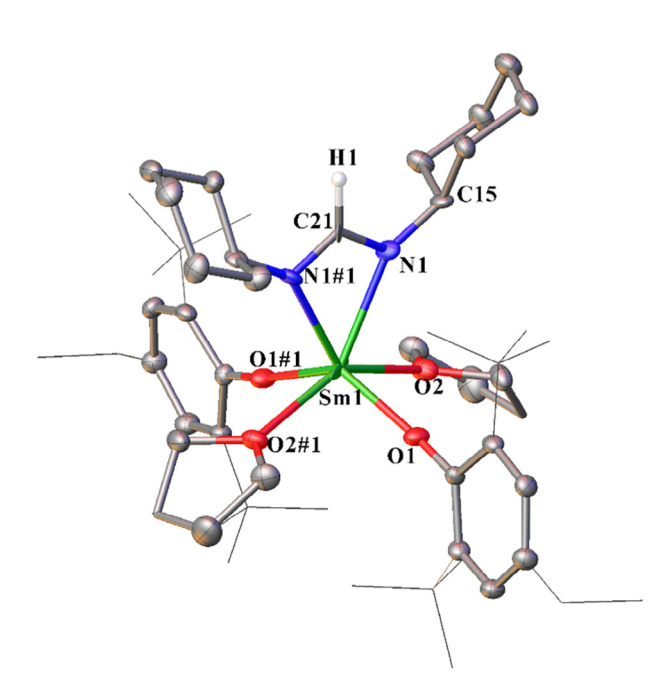


**Figure 2.** Molecular diagram of complex **2.** Hydrogen atoms (except for the hydrogen in the formamidinate fragment), as well as two lattice thf molecules are omitted for clarity. *Tert*-butyl and ethyl groups were drawn as wireframe for clarity.

O1,O2 at Sm1 and O3,O4 at Sm2). Each metal atom adopts a pseudo-trigonal-planar geometry if the oxalamidinate ligands are considered point donors (through C4 and C50). The phenolate groups are positioned above and below the plane formed by the Sm, two nitrogen atoms, and one of the central carbon atoms of the oxalamidinate ligand, oriented to minimize interactions with the isopropyl groups.

The two planes formed by the atoms Sm1, N1, N2, C4 and Sm2, N3, N4, C50 are nearly perpendicular, with dihedral angle of 91.0(5)° between them while the trigonal planes are also approximately orthogonal (dihedral angle 85.3(3)°). This staggered arrangement minimizes interactions between the neighboring isopropyl groups. The central C—C bond length is characteristic of a single bond, while the C—N bond lengths in the  $C_2N_4$  unit fall between typical single and double bond lengths, indicating electronically delocalized  $CN_2$  units within the diamidinate moiety.

#### 3.2. The complex [Sm(OArEt)2(CyNC(H)NCy)(thf)2]·2thf (2)

The complex  $[Sm(OAr^{Et})_2CyNC(H)NCy)(thf)_2]\cdot 2thf$  crystallizes in the monoclinic  $P2_1/c$  space group, containing half of the molecule in the asymmetric unit. Because of the quality of the structure, it is discussed only for connectivity. The samarium atom is six-coordinate, bonded to two  $OAr^{Et}$  ligands (through O1 and O1#1), two thf molecules (through O2 and O2#1), and two nitrogen atoms (through N1 and N1#1) from the chelating formamidinate fragment (Figure 2). The geometry around the samarium center is near pseudo square pyramidal, considering the  $\kappa(N,N')$  formamidinate ligand as a single-point donor from the central carbon atom of the 1,3-diazaallyl unit. Despite

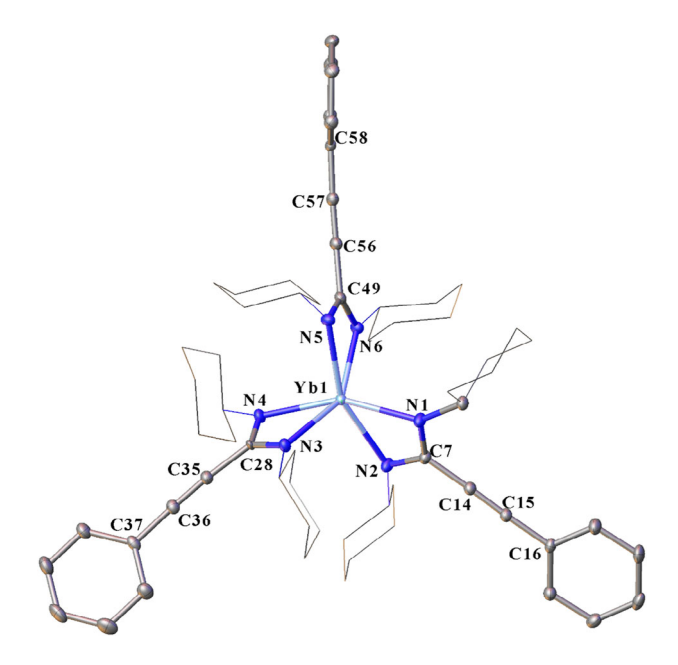


**Figure 3.** Molecular diagram of complex **3.** Hydrogen atoms along with two lattice thf molecules are omitted for clarity. Cyclohexyl rings were drawn as wireframe for clarity. Selected bond lengths (Å): Yb1–N1 2.3179(15), Yb1–N2 2.3366(15), Yb1–N3 2.3358(16), Yb1–N4 2.3236(15), Yb1–N5 2.3183(15), Yb1–N6 2.3224(15), N1–C7 1.334(2), N2–C7 1.328(2), N6–C49 1.332(2), N5–C49 1.332(2), N3–C28 1.317(2), N4–C28 1.350(2), C14–C15 1.193(3), C35–C36 1.196(3), C56–C57 1.194(3).

the limitation of the crystallographic data, they still establish proof of concept of the synthetic utility of the reaction giving 2 (Scheme 1).

#### 3.3. The complex [Yb<sup>III</sup>{CyNC(C≡CPh)NCy}<sub>3</sub>]·2thf (3)

The six coordinated complex **3** crystallizes in the triclinic *P-1* space group, adopting a pseudo-trigonal planar geometry if the phenylethynyl-substituted amidinate ligands are considered to be point donors located at the central carbon atoms. The complex has six nitrogen atoms from three  $\kappa(N,N')$  amidinate CyNC(C $\equiv$ CPh)NCy ligands, binding through N1,2, N3,4 and N5,6, which are arranged in a three-vane propeller configuration. The C $\equiv$ CPh groups, bound to the carbon atom of the CyNCNCy backbone are linear, with the Ph group positioned furthest from the metal (Figure 3).

The C—N bond lengths in the amidinate groups are nearly equivalent and significantly shorter than typical C—N single bonds, [35] suggesting that the  $\pi$  electrons of the C=N double bonds are delocalized across the N—C—N unit. The Yb—N distances of Cy-substituted nitrogen atoms fall between the typical Yb—N single bond lengths and donor N:— Yb bond lengths, which range from 2.19–2.69 Å.[16,36–38] In particular, they are similar to but marginally shorter than those (2.328(4)–2.354(5)Å)[23] of six coordinate [Yb(EtForm)<sub>3</sub>].2thf (EtForm = N,N'-bis(2,6-diethylphenyl)formamidinate), suggesting comparable steric demands between the present amidinate ligand and the bulky fomamidinate EtForm. The C=C bond lengths are close to those (1.204(2) and 1.206(2) Å) of diphenylacetylene.[39]

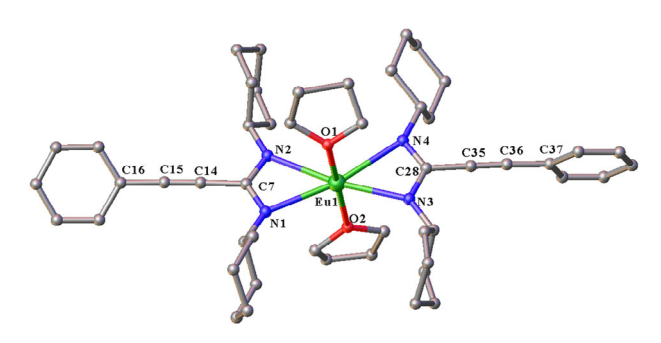


**Figure 4.** Molecular diagram of complex **4.** Hydrogen atoms are omitted for clarity. Selected bond lengths (Å): Eu1–O1 2.535(5), Eu1–O2 2.538(5), Eu1–N1 2.546(5), Eu1–N2 2.611(6), Eu1–N3 2.520(6), Eu1–N4 2.616(5), N1–C7 1.312(9), N2–C7 1.328(8), N3–C28 1.331(8), N4–C28 1.315(8), C14–C15 1.188(8), C35–C36 1.189(8).

#### 3.4. The complex $[Eu\{CyNC(C \equiv CPh)NCy\}_2(thf)_2]$ (4)

Complex 4 crystallizes in the monoclinic system, space group  $P2_1/c$ . The molecular structure is depicted in Figure 4. In the monomeric complex, the Eu atom is six-coordinate, with four N atoms from chelating amidinates fragments (binding through N1,2 and N3,4) coordinating in a  $\kappa$ -N,N'-fashion and two trans-thf donor molecules (O1 and O2; O1-Eu-O2 174.7(2)°). The coordination geometry is pseudo-square planar, when regarding the  $\kappa$ -N,N'-amidinate CyNC(C $\equiv$ CPh)NCy ligands occupying a single coordination site at the central carbon atoms (C7 and C28) of the NCN fragments. The europium—nitrogen bond lengths in complex 4 are longer than those in complex 3 by 0.25 Å, which is less than the 0.30 Å expected from the ionic radius difference between six coordinate Eu<sup>2+</sup> and six coordinate Yb<sup>3+</sup>.[40] This implies greater crowding in 3 than expected for the reduction in size. As for 3, the  $C \equiv C$  bond lengths are near those of diphenylacetylene.[39]

## 3.5. The structure of [Sm(OArEt)2(thf)3].PhMe

The structure of the reactant aryl oxide, prepared by metathesis from  $Sml_2(thf)_2$ , was also determined. It crystallizes in the monoclinic space group  $P2_{1/C}$  as a monomeric five coordinate (low coordination number) complex, analogous to several  $[Ln(OAr^{Me})_2(thf)_3]$  (Ln = Sm, Eu, Yb;  $OAr^{Me} = 2$ ,6-di-*tert*-butyl-4-methylphenolate) complexes, [41-44] and isomorphous with  $[Sm(OAr^{OMe})_2(thf)_3]$ .thf  $(OAr^{OMe} = 2$ ,6-di-*tert*-butyl-4-methoxyphenolate), [45] despite the different 4-substitutent (though similar chain length) and solvent of crystallization (Figure 5). The Reedijk parameter [46] is 0.54 indicating a stere-ochemistry essentially midway between square pyramidal and trigonal bipyramidal, but just favoring the latter. The Sm—O bond lengths are comparable with those of the isomorph. [45]

#### 4. Conclusions

The divalent samarium bis(phenoxide) complex [Sm(OAr<sup>Et</sup>)<sub>2</sub> (thf)<sub>3</sub>]-PhMe exhibits differing reductive reactivity with

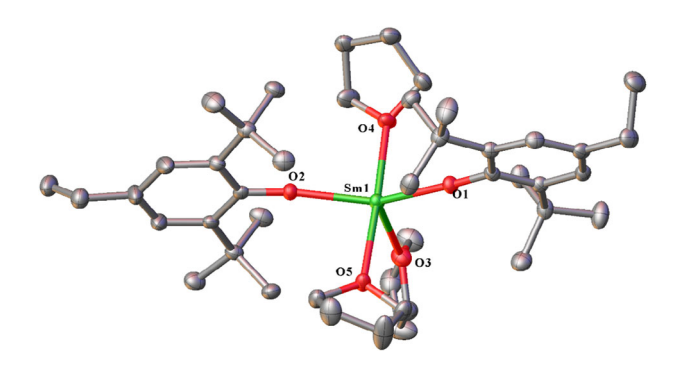


**Figure 5.** Molecular diagrams of  $[Sm(OAr^{Et})_2(thf)_3]$ -PhMe. Hydrogen atoms and lattice solvents are omitted for clarity. Selected bond lengths (Å): Sm1–O1 2.3202(15), Sm1–O2 2.3351(15), Sm1–O3 2.5434(18), Sm1–O4 2.5618(16), Sm1–O5 2.5833(16).

carbodiimides, depending on steric factors, and not insertion into the Sm-O bonds. With the less bulky N,N'bis(diisopropylcarbodiimide), one electron reduction and coupling yields a bimetallic oxalamidinatosamarium(III) complex 1, whereas the bulkier N,N'-dicyclohexylcarbodiimide gives the mononuclear formamidinatosamarium(III) complex 2. On the other hand, insertion reactions dominate on reaction of bis(phenylethynyl)lanthanoid(II) species,  $Ln(CCPh)_2$  (Ln = Eu, Yb), generated in situ from Ln metal and Hg(CCPh)<sub>2</sub>, with N,N'-dicyclohexylcarbodiimide. Whilst Eu(CCPh)<sub>2</sub>, gives a divalent C-phenylethynylamidinate,  $[Eu{CyNC(C \equiv CPh)NCy}_2(thf)_2]$  (4), the ytterbium analogue yields trivalent  $[Yb^{II}\{CyNC(C\equiv CPh)NCy\}_3]\cdot 2thf$  (3). Since the redox transmetallation between Yb metal and Hg(CCPh)2 is known to yield divalent Yb(CCPh)2, an additional oxidation and insertion step must be involved in the current reaction. Thus, carbodiimide reactions with divalent lanthanoid species provide a wide variety of outcomes.

#### 5. Experimental Section

#### 5.1. General

The compounds prepared in this work are extremely sensitive to air and moisture, and all manipulations were performed under a nitrogen atmosphere using vacuum–nitrogen line techniques, and a glove box with purified nitrogen, ensuring rigorous exclusion of air and water. Lanthanoid metals were obtained from Molycorp or Eutectix. Large chunks were filed in the drybox before use. Solvents (thf, C<sub>6</sub>D<sub>6</sub>, toluene) were pre-dried by distillation over sodium or sodium benzophenone ketyl and stored under a nitrogen atmosphere over 4 Å molecular sieves.

The following reagents were commercially available and used without further purification: 2,6-di-*tert*-butyl-4-ethylphenol (HOAr<sup>Et</sup>), 1,2-diiodoethane, *N*,*N*"-dicyclohexylcarbodiimide (DCC) and *N*,*N*"-diisopropylcarbodiimide (DIC). Bis(phenylethynyl)mercury<sup>[47]</sup> and Sml<sub>2</sub>(thf)<sub>2</sub><sup>[48]</sup> were prepared using literature methods. Infrared spectra (4000–400 cm<sup>-1</sup>) were obtained as Nujol mulls between NaCl plates with a Nicolet iS FTIR spectrometer. <sup>1</sup>H spectra were recorded on a Bruker 400 MHz instrument, with chemical shifts referenced against residual solvent peaks. Microanalyses were conducted by the Elemental Analysis Service, London Metropolitan University, with all samples sealed in tubes under nitrogen before transport. Metal

Chemistry Europe

European Chemical Societies Publishing

analyses were performed by using EDTA titrations with xylenol orange as the indicator, following acid digestion and buffering with hexamethylenetatramine. Melting points were determined in sealed glass capillaries under nitrogen and are uncalibrated.

CCDC 2426980 for compound 1, 2426981–2426982 for compounds 3 and 4, 2426983 for compound [Sm(OAr<sup>Et</sup>)<sub>2</sub>(thf)<sub>3</sub>]·PhMe, contain the supplementary crystallographic data for this paper. These data can be obtained free of charge from The Cambridge Crystallographic Data Centre via www.ccdc.cam.ac.uk/data\_request/cif.

#### 5.2. Syntheses

## 5.2.1. $[(OAr^{Et})_2Sm(\mu-C_2N_4iPr_4)Sm(OAr^{Et})_2]\cdot 2PhMe$ (1)

A solution of N,N -di-isopropyl-carbodiimide (0.16 mL, 1.00 mmol) in toluene (10 mL) was added with stirring at room temperature to a dark red solution of [Sm(OAr<sup>Et</sup>)<sub>2</sub>(thf)<sub>3</sub>]·PhMe (0.926 g, 1.00 mmol) in toluene. The color gradually changed to light yellow, and the mixture was stirred continuously for 3 days. The resulting solution was filtered using a filtration cannula and concentrated in vacuo to approximately 10 mL and stored at -25°C for 1 week, to yield lightyellow crystals. Yield: 0.43 g (51%). m.p. 138-140 °C (dec.). Elemental analysis calculated (%) for  $C_{92}H_{144}N_4O_4Sm_2$  (MW: 1670.87  $gmol^{-1}):$ on fresh crystals Sm 17.99; found (%) Sm 17.26. Microanalysis (after transport to London) calculated (%) for C<sub>85</sub>H<sub>136</sub>N<sub>4</sub>O<sub>4</sub>Sm<sub>2</sub> (MW 1578.77 gmol<sup>-1</sup>, loss of 1 PhMe of crystallization) C 64.67, H 8.68, N 3.55 Found (%) C 65.00; H 8.86; N 3.74. IR (Nujol, cm<sup>-1</sup>): 3064w, 2116s, 1758 m, 1643 m, 1604 m, 1571 m, 1495w, 1383 m, 1350 m, 1326w, 1311w, 1169w, 1140w, 1121s, 1081w, 1060w, 1009s, 910s, 891s, 874s, 832s, 795s, 781w, 764 m, 729s, 694s, 639w, 535w. <sup>1</sup>H NMR (400 MHz, C<sub>6</sub>D<sub>6</sub>, 25°C, ppm):  $\delta = 8.05-8.48$  (m, 8H,  $C_6H_2$ ), 7.05 (m, 5H, ArH-toluene), 3.15-3.40 (m, 8H, CH<sub>2</sub>), 2.58 (m, 4H, CH), 2.11 (m, 3H, CH<sub>3</sub>-toluene), 0.3-2.04 (m, 36H, CH<sub>3</sub>-Et, iPr), -0.42-0.79 (m, 72H, CH<sub>3</sub>-tBu) with one lattice PhMe lost.

#### 5.2.2. $[Sm(OAr^{Et})_2(CyNC(H)NCy)(thf)_2] \cdot 2thf$ (2)

A solution of N,N'-dicyclohexylcarbodiimide (DCC) (0.10 g, 0.48 mmol) in thf (10 mL) was added with stirring at room temperature to a dark red solution of [Sm(OAr<sup>Et</sup>)<sub>2</sub>(thf)<sub>3</sub>]·PhMe (0.30 g, 0.48 mmol) in thf. The color gradually changed to light yellow, and the mixture was stirred continuously for 3 days. The resulting solution was filtered using a filtration cannula and concentrated in vacuo to approximately 10 mL and stored at -25°C for 1 week, to yield light-yellow crystals. Yield: 0.16 g (30%). m.p. 110°C (dec.). Elemental analysis calculated (%) for  $C_{61}H_{105}N_2O_6Sm$  (MW: 1112.85 gmol<sup>-1</sup>): on fresh crystals Sm 13.51; found (%) Sm 13.60. Microanalysis (after transport to London) calculated (%) for C<sub>53</sub>H<sub>89</sub>N<sub>2</sub>O<sub>4</sub>Sm (MW 968.67 gmol<sup>-1</sup>, loss of 2 thf of crystallization): C 65.72; H 9.26; N 2.89. Found (%) C 64.07; H 8.99; N 2.97. IR (Nujol, cm<sup>-1</sup>): 2120s, 1753w, 1640s, 1604w, 1544s, 1459 m, 1419 m, 1384 m, 1358w, 1325 m, 1259 m, 1234 m, 1212w, 1158w, 1120 m, 1072 m, 1024w, 910w, 890w, 873 m, 821s, 793s, 721w. <sup>1</sup>H NMR (400 MHz, C<sub>6</sub>D<sub>6</sub>, 25°C, ppm): Satisfactory integrations could not be obtained (see Figure S2).  $\delta = 8.15$  (s, 4H, ArH), 7.98 (s, 1H, NCHN), 3.16-0.70 (m, CH<sub>3</sub>-tBu, CH<sub>3</sub>-Et, CH<sub>2</sub>-Et, CyNCNCy Hs overlapped by CH<sub>2</sub>-thf resonance) with both lattice thf lost.

# 5.2.3. General procedure for 3 and 4

A Schlenk flask was charged with  $Hg(PhCC)_2$  (0.605 g, 1.5 mmol) and excess Yb metal filings (0.52 g, 3.0 mmol) (3)/Eu metal filings (0.455 g, 3.0 mmol) (4), followed by N,N'-dicyclohexylcarbodiimide

(DCC) (0.619 g, 3.0 mmol) added inside a drybox. Anhydrous thf (15 mL) was then added and stirred at room temperature for 3 days. After allowing the unreacted lanthanoid metal and mercury suspension to settle, the supernatants were filtered using a filtration cannula. The resulting solutions were concentrated in vacuo to approximately 10 mL and left to stand at room temperature to crystallize.

#### 5.2.4. $[Yb\{CyNC(C \equiv CPh)NCy\}_3] \cdot 2thf(3)$

Yellow crystals (0.80 g, 64%); m.p. 195°C–200°C. Elemental analysis for  $C_{71}H_{97}N_6O_2$ Yb (MW: 1239.61 gmol $^{-1}$ ): Calculated (%) C 68.79; H 7.89; N 6.78; Yb 13.96; Found (%) C 68.58; H 7.95; N 6.85; Yb 13.72. IR (Nujol, cm $^{-1}$ ): 2666w, 2209s, 1968w, 1947w, 1897w, 1877w, 1799w, 1750w, 1671 m 1597 m, 1573 m, 1558w, 1311w, 1257s, 1245s, 1191s, 1171s, 1137s, 1073s, 1026 m, 995s, 964w, 913s, 898s, 887s, 843s, 805 m, 755s, 722w, 702 m, 688s, 676w, 628s, 529w.  $^1$ H NMR (400 MHz,  $C_6D_6$ , 25°C, ppm):  $\delta$  = 13.79 (s, 3H, ArH), 7.43–6.73 (m, ArH overlap with  $C_6D_6$ ), 3.94–1.50 (m, 86H, 60 CH<sub>2</sub>-CyNCNCy, 6 CH- CyNCNCy, 20 thf), -0.20 (s, 8H, CH<sub>2</sub>-thf), -13.80 (s, 8H, CH<sub>2</sub>-thf).

#### 5.2.5. $[Eu\{CyNC(C \equiv CPh)NCy\}_2(thf)_2]$ (4)

Red crystals (0.51 g, 56%); m.p.  $133^{\circ}$ C- $135^{\circ}$ C. Elemental analysis for  $C_{50}H_{70}EuN_4O_2$  (MW: 911.08 gmol $^{-1}$ ): calculated (%) C 65.91; H 7.74; N 6.15; Eu 16.68; found (%) C 65.22; H 7.97; N 6.03 Eu 15.90. IR (Nujol, cm $^{-1}$ ): 2122s, 1953 m, 1883w, 1757w, 1686w, 1655w, 1596 m, 1572w, 1560w, 1545 m, 1379w, 1356w, 1319w, 1303w, 1256s, 1240w, 1165s, 1126 m, 1110 m, 1070s, 1043s, 991 m, 915s, 886s, 843 m, 796 m, 756s, 721w, 691s, 670s, 615s, 592 m, 526w.

## 5.2.6. $[Sm(OAr^{Et})_2(thf)_3] \cdot PhMe$

Under a N<sub>2</sub> atmosphere, tetrahydrofuran (30 mL) was distilled onto 2,6-di-tert-butyl-4-ethylphenol (HOArEt) (2.3438 g, 10.0 mmol) and excess potassium (0.44 g, 11.0 mmol). After 4 h, this solution was directly filtered and added dropwise to a deep blue solution of  $[Sm(I)_2(thf)_2]$  (2.74 g, 5.0 mmol), in tetrahydrofuran (20 mL). The resulting deep red solution was stirred overnight. The solution was then evaporated to dryness, dissolved in toluene (30 mL) and stirred for 1 h. Filtration, followed by removal of all volatiles in vacuo, yielded a red powder, which was subsequently extracted into toluene (10 mL) and left at -25°C for several days to produce deep red crystals. Yield: 2.04 g (66%). m.p. 190°C (dec.). Elemental analysis calculated (%) for  $C_{51}H_{82}O_5Sm$  (MW: 925.55 gmol<sup>-1</sup>): on fresh crystals Sm 16.99; found (%) Sm 16.24. Microanalysis (after transport to London) calculated (%) for  $C_{32}H_{50}O_2Sm$  (MW 617.10 gmol $^{-1}$ , loss of 3 thf and 1 PhMe): C 62.28; H 8.17. Found (%) C 60.78; H 8.39. IR (Nujol, cm<sup>-1</sup>): 1757 m, 1603 m, 1559w, 1544w, 1495w, 1459s, 1418s, 1379s, 1346 m, 1324s, 1260s, 1234s, 1212 m, 1120 m, 1083w, 1031s, 910 m,  $\,$ 874s, 821s, 793s, 729s, 696s, 664w. <sup>1</sup>H NMR (400 MHz, C<sub>6</sub>D<sub>6</sub>, 25°C, ppm):  $\delta = 8.14$  (s, 4H, H<sub>3.5</sub>(OAr<sup>Et</sup>)), 7.11 (m, 5H, CH(toluene)), 3.17(q, 4H, CH<sub>2</sub>(OAr<sup>Et</sup>)), 2.50 (m, 2H, CH<sub>2</sub>-thf), 2.12 (m, 3H, CH<sub>3</sub>(Toluene)), 1.78 (t, 6H,  $CH_3(OAr^{Et})$ ), 1.40 (s, 6H,  $C(CH_3)_3(OAr^{Et})$ ), 0.86 (s, 30H,  $C(CH_3)_3(OAr^{Et})$ , -0.93 (m, 2H,  $CH_2$ -thf) with 2.5 thf lost.

# Acknowledgments

GBD and PCJ gratefully acknowledge the ARC for funding (DP230100112).

Chemistry Europe

European Chemical Societies Publishing

Open access publishing facilitated by James Cook University, as part of the Wiley - James Cook University agreement via the Council of Australian University Librarians.

#### Conflicts of Interest

The authors declare no conflict of interest.

# **Data Availability Statement**

The data that support the findings of this study are available from the corresponding author upon reasonable request.

**Keywords:** aryloxide · carbodiimide · insertion · lanthanoids · redox transmetallation · reductive coupling

- M. F. Lappert, B. Prokai, Advances in Organometallic Chemistry, Vol. 5, 1st ed., Academic Press, New York, 1967.
- [2] G. B. Deacon, C. M. Forsyth, P. C. Junk, J. Wang, *Inorg. Chem.* 2007, 46, 10022.
- [3] L. Yang, Y. Qu, J. Wang, W. Xu, Y. Zhao, X. J. Yang, Chem.-Eur. J. 2023, 29, e202301266.
- [4] J. Louie, Curr. Org. Chem. 2005, 9, 605.
- [5] Y. Wang, W. X. Zhang, Z. Xi, Chem. Soc. Rev. 2020, 49, 5810.
- [6] Z. Li, R. J. Mayer, A. R. Ofial, H. Mayr, J. Am. Chem. Soc. 2020, 142, 8383.
- [7] L. Xu, W. X. Zhang, Z. Xi, Organometallics 2015, 34, 1787.
- [8] C. Alonso-Moreno, F. Carrillo-Hermosilla, A. Garcés, A. Otero, I. López-Solera, A. M. Rodríguez, A. Antiñolo, Organometallics 2010, 29, 2789.
- [9] F. Zeng, H. Alper, Org. Lett. 2010, 12, 1188.
- [10] R. T. Yu, T. Rovis, J. Am. Chem. Soc. 2008, 130, 3262.
- [11] M. L. Cole, G. B. Deacon, C. M. Forsyth, P. C. Junk, D. P. Ceron, J. Wang, Dalton Trans. 2010, 39, 6732.
- [12] J. Zhang, R. Ruan, Z. Shao, R. Cai, L. Weng, X. Zhou, Organometallics. 2002. 21, 1420.
- [13] F. T. Edelmann, Adv. Organomet. Chem. 2008, 57, 183.
- [14] G. Chandra, A. D. Jenkins, M. F. Lappert, R. C. Srivastava, *J. Chem. Soc. A* 1970, 2550.
- [15] C. Pi, Z. Zhang, Z. Pang, J. Zhang, J. Luo, Z. Chen, L. Weng, X. Zhou, Organometallics 2007, 26, 1934.
- [16] J. Zhang, R. Cai, L. Weng, X. Zhou, J. Organomet. Chem. 2003, 672, 94.
- [17] A. A. Trifonov, D. M. Lyubov, E. A. Fedorova, G. G. Skvortsov, G. K. Fukin, Y. A. Kurskii, M. N. Bochkarev, G. A. Razuvaev, Russ. Chem. Bull. 2006, 55, 435.
- [18] W. J. Evans, J. W. Grate, I. Bloom, W. E. Hunter, J. L. Atwood, J. Am. Chem. Soc. 1985, 107, 105.
- [19] W. J. Evans, R. A. Keyer, J. W. Ziuer, J. Organomet. Chem. 1990, 394, 87.
- [20] Z. Hou, A. Fujita, Y. Zhang, T. Miyano, H. Yamazaki, Y. Wakatsuki, 1998, 120, 754

- [21] M. Deng, Y. Yao, Y. Zhang, Q. Shen, ChemComm 2004, 2742.
- [22] G. B. Deacon, A. J. Koplick, W. D. Raverty, D. G. Vince, J. Organomet. Chem. 1979, 182, 121.
- [23] M. L. Cole, G. B. Deacon, C. M. Forsyth, P. C. Junk, K. Konstas, J. Wang, Chem.-Eur. J. 2007, 13, 8092.
- [24] M. Salehisaki, N. E. Rad, G. B. Deacon, J. Wang, Z. Guo, P. C. Junk, *Inorg. Chim. Acta* 2022, 539, 120997.
- [25] G. J. Moxey, A. J. Blake, W. Lewis, D. L. Kays, Eur. J. Inorg. Chem. 2015, 5892
- [26] R. P. Kelly, T. D. M. Bell, R. P. Cox, D. P. Daniels, G. B. Deacon, F. Jaroschik, P. C. Junk, X. F. Le Goff, G. Lemercier, A. Martinez, J. Wang, D. Werner, Organometallics 2015, 34, 5624.
- [27] H. Sitzmann, T. Dezember, O. Schmitt, F. Weber, G. Wolmershäuser, M. Ruck, Z. Anorg. Allg. Chem. 2000, 626, 2241.
- [28] L. H. J. Lajunen, G. R. Choppin, Rev. Anal. Chem. 1989, 9, 91.
- [29] D. P. Daniels, G. B. Deacon, D. Harakat, F. Jaroschik, P. C. Junk, *Dalton Trans.* 2012, 41, 267.
- [30] L. Hirneise, C. Maichle-Mössmer, R. Anwander, Inorg. Chem. 2021, 60, 18211.
- [31] G. B. Deacon, A. J. Koplick, T. D. Tuong, Aust. J. Chem. 1982, 35, 941.
- [32] L. J. Bellamy, The Infrared Spectra of Complex Molecules, Advances in Infrared Group Frequencies, Vol. 2, Chapman & Hall, London, 1968.
- [33] J. D. Wilkins, J. Organomet. Chem. 1974, 80, 349.
- [34] Lewis, J., Miller, J. R., Richards, R. L., Thompson, A., J. Chem. Soc. 1965, 5850.
- [35] F. H. Allen, O. Kennard, D. G. Watson, L. Brammer, A. G. Orpen, R. Taylor, J. Chem. Soc., Perkin Trans. 2 1987, S1.
- [36] W. J. Evans, D. K. Drummond, L. R. Chamberlain, R. J. Doedens, S. G. Bott, H. Zhang, J. L. Atwood, J. Am. Chem. Soc. 1988, 110, 4983.
- [37] X.-G. Zhou, Z.-E. Huang, R.-F. Cai, L.-X. Zhang, X.-F. Hou, X.-J. Feng, X.-Y. Huang, J. Organomet. Chem. 1998, 563, 101.
- [38] X. G. Zhou, Z. E. Huang, R. F. Cai, L. B. Zhang, L. X. Zhang, X. Y. Huang, Organometallics 1999, 18, 4128.
- [39] R. Thomas, S. Lakshmi, S. K. Pati, G. U. Kulkarni, J. Phys. Chem. B 2006, 110, 24674.
- [40] R. D. Shannon, Acta Crystallogr., Sect. A 1976, 32, 751.
- [41] J. R. van den Hende, P. B. Hitchcock, S. A. Holmes, M. F. Lappert, W.-P. Leung, T. C. W. Mak, S. Prashar, *Dalton Trans.* 1995, 1427.
- [42] G.-Z. Qi, Q. Shen, Y.-H. Lin, Acta Crystallogr., Sect. C 1994, 50, 1456.
- [43] G. B. Deacon, P. B. Hitchcock, S. A. Holmes, M. F. Lappert, P. MacKinnon, R. H. Newnham, J. Chem. Soc., Chem. Commun. 1989, 935.
- [44] S. Beaini, G. B. Deacon, M. Hilder, P. C. Junk, D. R. Turner, Eur. J. Inorg. Chem. 2006, 2006, 3434.
- [45] G. B. Deacon, G. D. Fallon, C. M. Forsyth, S. C. Harris, P. C. Junk, B. W. Skelton, A. H. White, *Dalton Trans.* 2006, 802.
- [46] A. W. Addison, T. N. Rao, J. Reedijk, J. van Rijn, G. C. Verschoor, *Dalton Trans.* 1984, 1349.
- [47] B. G. Eglinton, W. Mccrae, J. Chem. Soc. 1963, 2295.
- [48] P. Girard, J. L. Namy, B. Kagan, J. Am. Chem. Soc. 1980, 102, 2693.

Manuscript received: February 26, 2025 Revised manuscript received: March 19, 2025 Version of record online: April 9, 2025